

## Evolution of a magnetic state in $\text{YbCu}_{5-x}\text{Ga}_x$

E. Bauer, Le Tuan, R. Hauser, E. Gratz, T. Holubar, G. Hilscher, H. Michor, and W. Perthold  
*Institut für Experimentalphysik, Technische Universität Wien, A-1040 Wien, Austria*

C. Godart

*CNRS Meudon, F-92195 Meudon, France*  
*and Laboratoire pour l'Utilisation du Rayonnement Electromagnétique,*  
*CNRS, Université de Paris Sud, F-91405 Orsay, France*

E. Alleno

*CNRS Meudon, F-92195 Meudon, France*

K. Hiebl

*Institut für Physikalische Chemie, Universität Wien, A-1090 Wien, Austria*

(Received 7 March 1995)

Substitutions of Cu by Ga in  $\text{YbCu}_5$  stabilize the hexagonal  $\text{CaCu}_5$  structure and cause a crossover from a divalent behavior of the Yb ion in  $\text{YbCu}_5$  to an almost  $3+$  state of Yb in  $\text{YbCu}_3\text{Ga}_2$ . This gain of magnetism is accompanied by a noticeable enhancement of the electronic contribution to the specific heat. External pressure transforms those compounds, exhibiting intermediate valence, to a state which is best described in terms of the Kondo lattice model.

### I. INTRODUCTION

The series  $\text{YbCu}_x$  has been investigated in detail, leading to, at least, five intermetallic compounds.<sup>1</sup> Three of them ( $\text{YbCu}$ ,  $\text{YbCu}_2$ , and  $\text{YbCu}_5$ ) are characterized by an intermediate valence behavior, while the others ( $\text{Yb}_2\text{Cu}_7$  and  $\text{Yb}_2\text{Cu}_9$ ) show Curie-Weiss behavior, where the Curie constant indicates a  $3+$  state of the Yb ions.

Particularly,  $\text{YbCu}_5$  is of interest as a starting material for a series of compounds with various interesting low-temperature features. These range from intermediate valence to the Kondo regime exhibiting both long-range magnetic order with reduced moments and paramagnetism down to the lowest temperatures. The unusual large Kondo temperature  $T_K$  of the cubic compound  $\text{YbCu}_4\text{Ag}$  ( $T_K \approx 150$  K) (Refs. 2–6) hinders magnetic order whereby crystal field splitting appears to be of minor importance. On the contrary, crystal field splitting and long-range magnetic order dominate the ground state properties of  $\text{YbCu}_4\text{Al}$  due to a small value of  $T_K$ .<sup>7–9</sup> Previously, it has been shown that a substitution of Cu by Al leaves the hexagonal  $\text{CaCu}_5$  crystal structure unchanged.<sup>10–13</sup> The limiting composition of this solid solution was found to be  $\text{YbCu}_{2.9}\text{Al}_{2.1}$ .<sup>14</sup> This substitution is responsible for a crossover from an almost divalent behavior of the Yb ion in  $\text{YbCu}_5$  to a trivalent state of Yb in  $\text{YbCu}_3\text{Al}_2$ . Additionally, long-range magnetic order appears. Both the ordering temperature  $T_N$  and the magnitude of the Yb moments in the crystal field ground state increase with growing Al content. While  $T_N$  rises from about 1 K in  $\text{YbCu}_{3.25}\text{Al}_{1.75}$  to 2 K for  $\text{YbCu}_3\text{Al}_2$ ,

the magnitude of the Yb moment grows from about  $1\mu_B$  in  $\text{YbCu}_{3.25}\text{Al}_{1.75}$  to  $2\mu_B$  in  $\text{YbCu}_3\text{Al}_2$ .<sup>12,13,15</sup> Simultaneously, the paramagnetic Curie temperature changes from about  $-340$  K deduced for  $\text{YbCu}_4\text{Al}$  to  $-17$  K as obtained for  $\text{YbCu}_3\text{Al}_2$ .<sup>12</sup>

The aim of the present paper is a study of the crystallographic section  $\text{YbCu}_{5-x}\text{Ga}_x$  which is found to crystallize also in the hexagonal  $\text{CaCu}_5$  structure. The stability range for compounds with the hexagonal unit cell extends at least up to  $x = 2$ . Associated with the Cu/Ga substitution is a dramatic change of the physical properties indicated by susceptibility measurements,  $L_{\text{III}}$ -absorption edge measurements, the investigation of the specific heat, and by transport properties which have been studied as a function of temperature and applied pressure up to about 70 kbar.

### II. EXPERIMENTAL DETAILS

Polycrystalline  $\text{YbCu}_{5-x}\text{Ga}_x$  samples, with  $0 \leq x \leq 2$  were prepared by high-frequency melting under argon atmosphere and subsequently annealed for 14 days at  $700^\circ\text{C}$ . The phase purity and the lattice parameters have been determined using a standard x-ray diffractometer with the  $K\alpha$  radiation of a Cr tube. All samples are found to crystallize in the hexagonal  $\text{CaCu}_5$  structure. In order to obtain phase purity also for  $\text{YbCu}_5$ , this compound has been prepared with Cu excess. The deduced lattice parameters  $a$  and  $c$  (collected in Table I) show that the volume  $V$  of the unit cell increases with rising Ga content. In parallel, the lattice parameter  $a$  grows,

TABLE I. Crystal structure, lattice parameters  $a$  and  $c$ , volume of the crystallographic unit cell  $V$ , Pauli contribution  $\chi_0$ , Curie constant  $C$ , effective magnetic moment  $\mu_{\text{eff}}$ , paramagnetic Curie temperature  $\theta_p$ , valency  $\nu$ , specific heat contribution  $c_p/T(T \rightarrow 0)$ , and electronic contribution to the specific heat  $\gamma^{\text{HT}}$  observed from a high-temperature extrapolation.

YbCu <sub>5-x</sub> Ga <sub>x</sub>	$x = 2$	$x = 1.5$	$x = 1$	$x = 0$
Structure	CaCu <sub>5</sub>	CaCu <sub>5</sub>	CaCu <sub>5</sub>	CaCu <sub>5</sub>
$a$ [Å]	5.1134(9)	5.077(1)	5.0672(8)	4.994(9)
$c$ [Å]	4.119(2)	4.129(1)	4.1216(7)	4.126(2)
$3V$ [Å <sup>3</sup> ]	$\sim 279.85$	$\sim 276.50$	$\sim 274.96$	$\sim 267.35$
$\chi_0$ [emu/mol]	0.000067	—	—	—
$C$ [emuK/mol]	2.608	no CW <sup>a</sup>	no CW <sup>a</sup>	no CW <sup>a</sup>
$\mu_{\text{eff}}$ [ $\mu_B$ ]	4.56	no CW <sup>a</sup>	no CW <sup>a</sup>	no CW <sup>a</sup>
$\theta_p$ [K]	-123	-430 <sup>b</sup>		
$T_{\text{ex}} = E_{\text{ex}}/k_B$ [K]		-525	-1050	
$T_{sf}$ [K]		115	170	
$\nu$ at 300 K	2.91		2.59	
$\nu$ at 10 K	2.83		2.50	
$c_p/T(T \rightarrow 0)$ [mJ/mol K <sup>2</sup> ]	180	75	40	13
$\gamma^{\text{HT}}$ [mJ/mol K <sup>2</sup> ]	63	22	3	2

<sup>a</sup>No Curie-Weiss behavior.

<sup>b</sup>Obtained from a linear extrapolation.

while  $c$  shows a faint tendency to decrease. A comparison of the observed intensity distribution of the x-ray pattern and that calculated with a computer program indicates that Ga preferentially occupies the 3( $g$ ) sites of the unit cell with  $P6/mmm$  symmetry. As the Ga concentration  $x$  exceeds the value  $x = 2$  the crystal structure becomes multiphase. This crystallographic situation resembles the crystallographic situation found previously for the series YbCu<sub>5-x</sub>Al<sub>x</sub>.<sup>12,13</sup>

The temperature-dependent magnetic susceptibility was investigated up to room temperature by means of a superconducting quantum interference device (SQUID) magnetometer. High-temperature measurements (300 K  $\leq T \leq$  900 K) were performed by a Faraday balance (SUS-10). X-ray-absorption spectroscopy (XAS) was performed at the French synchrotron radiation facility (LURE) in Orsay using the x-ray beam of the DCI storage ring (working at 1.85 GeV and  $\approx$  320 mA) on the extended x-ray-absorption fine-structure (EXAFS) D22 station. A double Si (311) crystal was used as a monochromator. Rejection of third-order harmonics was achieved with the help of two parallel mirrors adjusted to cut off energies higher than 10 keV. Experiments were carried out in the energy range 8080–9060 eV, which contains the  $L_{\text{III}}$  edge of Yb (and the  $K$  edge of Cu). Finely powdered samples were spread on an adhesive Kapton tape and four of such tapes were stacked together for preparing a sample layer of thickness sufficient enough to ensure a good signal. Moreover, this was also helpful in eliminating, to a good extent, any sample-free regions in the path of the radiation. X-ray-absorption spectra were measured at two fixed temperatures, 300 and 10 K. Specific heat measurements on samples of about 2 g were performed at temperatures from 1.5 K up to 60 K using a modified Nernst-step-heating technique. The electrical resistivity of bare-shaped samples was measured using a four-probe dc method in the temperature range from 1.5

K to room temperature. Two different methods to generate high pressure were applied. Up to 20 kbar a liquid pressure cell with a 4:1 methanol-ethanol mixture as pressure transmitter was used. Beyond 20 kbar, the Bridgman technique with Al<sub>2</sub>O<sub>3</sub> anvils and pyrophyllit gaskets was applied. Steatit served as pressure-transmitting medium. The absolute value of the pressure was determined from the superconducting transition of lead.<sup>16</sup>

### III. RESULTS AND DISCUSSION

#### A. Valence state of YbCu<sub>5-x</sub>Ga<sub>x</sub>

A characterization of the physical behavior and its change due to the Ga substitution is probably best seen from the study of the temperature-dependent magnetic susceptibility  $\chi(T)$ . Figure 1 shows  $\chi^{-1}$  vs  $T$  of various YbCu<sub>5-x</sub>Ga<sub>x</sub> compounds. The magnetic susceptibility  $\chi(T)$  of YbCu<sub>5</sub> and YbCu<sub>3</sub>Ga<sub>2</sub> is shown as an inset in this figure. While the susceptibility of the latter compound exhibits Curie-Weiss behavior, the former compound is characterized by an almost temperature-independent Pauli susceptibility with  $\chi_0 \approx 6 \times 10^{-4}$  emu/mol at room temperature. Pauli paramagnetism of YbCu<sub>5</sub> has already been reported by Iandelli and Palenzona.<sup>1</sup>

Owing to the substitution of Cu by Ga, the magnetic state of the Yb ion changes continuously from almost Yb<sup>2+</sup> in YbCu<sub>5</sub> to Yb<sup>3+</sup> in YbCu<sub>3</sub>Ga<sub>2</sub>. This crossover is clearly traced by a pronounced change of  $\chi(T)$  resulting in a Curie-Weiss behavior for YbCu<sub>3</sub>Ga<sub>2</sub> above about 50 K. An almost linear behavior of  $\chi^{-1}(T)$  is evident for the compound  $x = 1.5$  for temperatures higher than 250 K. On the contrary, YbCu<sub>4</sub>Ga exhibits a broad maximum in  $\chi^{-1}(T)$  between 4 K and room temperature. The

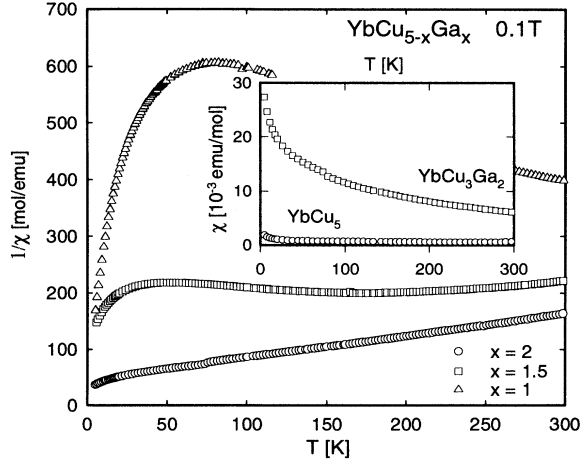


FIG. 1. Temperature-dependent magnetic susceptibility  $\chi$  of  $\text{YbCu}_{5-x}\text{Ga}_x$  compounds plotted as  $\chi^{-1}$  vs  $T$ . The inset shows  $\chi(T)$  of  $\text{YbCu}_5$  and  $\text{YbCu}_3\text{Ga}_2$ .

pronounced nonlinear behavior of  $\chi^{-1}(T)$  of  $\text{YbCu}_4\text{Ga}$  matches the results previously reported by Adroja *et al.*<sup>10</sup>

Analyzing the susceptibility data of  $\text{YbCu}_3\text{Ga}_2$  in a proper temperature range ( $T > 50$  K) with a modified Curie-Weiss law, i.e.,

$$\chi = \chi_0 + \frac{C}{T - \theta_p}, \quad (1)$$

yields information concerning the temperature-independent Pauli contribution  $\chi_0$ , the effective magnetic moment  $\mu_{\text{eff}}$  (deduced from the Curie constant  $C$ ), and the paramagnetic Curie temperature  $\theta_p$ . Results of a least squares fit according to the Eq. (1) are presented in Table I.  $\text{YbCu}_3\text{Ga}_2$  shows an effective magnetic moment  $\mu_{\text{eff}}$  close to that of the free ion value of  $\text{Yb}^{3+}$ . The absolute value of the paramagnetic Curie temperature  $\theta_p$  appears to be very large. This is most likely attributed to the Kondo interaction present in these compounds. In the absence of crystal field splitting,  $\theta_p$  is related to the Kondo temperature via  $T_K = m|\theta_p|$  with  $0.25 \leq m \leq 1$ , where  $m$  depends on the choice of the different theoretical models.<sup>20</sup> Consequently,  $T_K$  of  $\text{YbCu}_3\text{Ga}_2$  is also large. A linear extrapolation of  $\chi^{-1}(T)$  of  $\text{YbCu}_{3.5}\text{Ga}_{1.5}$  from the temperature range  $250 \text{ K} \leq T \leq 300 \text{ K}$  yields a temperature of about  $-440$  K. It seems therefore that  $T_K$  is strongly concentration dependent and decreases as the Yb moments acquire a more “magnetic” state.

To study the magnetic behavior of the compounds which do not obey a Curie-Weiss behavior in more detail, we have measured the susceptibility of  $\text{YbCu}_{3.5}\text{Ga}_{1.5}$  and of  $\text{YbCu}_4\text{Ga}$  up to 900 K. Results of these investigations are shown in Fig. 2. As indicated earlier by Klaase *et al.*,<sup>17,18</sup> the low-temperature susceptibility of Yb compounds may be dominated by oxide impurities. To correct for these impurities, we follow the procedure employed by Klaase *et al.*<sup>17,18</sup> There, it is assumed that the impurity type is  $\text{Yb}_2\text{O}_3$  and the other contributions are almost constant at low temperatures.<sup>17</sup> For

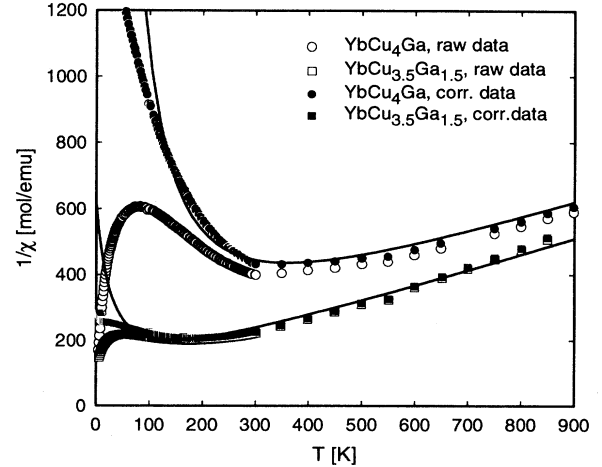


FIG. 2. Temperature-dependent magnetic susceptibility  $\chi$  of  $\text{YbCu}_{3.5}\text{Ga}_{1.5}$  and  $\text{YbCu}_4\text{Ga}$  plotted as  $\chi^{-1}$  vs  $T$ . The open and the solid symbols show the measured and corrected data (see text). The solid lines are least squares fits according to the ICF model.

$T > 150$  K, the susceptibility of  $\text{Yb}_2\text{O}_3$  is characterized by a Curie-Weiss behavior with an effective magnetic moment  $\mu_{\text{eff}} = (4.55 \pm 0.05)\mu_B$  and a paramagnetic Curie-temperature  $\theta_p = (-45 \pm 15)$  K.<sup>18</sup> However, for the correction procedure we used only the low-temperature data of the magnetic susceptibility of  $\text{Yb}_2\text{O}_3$ . The oxide contribution can then be subtracted from the observed  $\chi(T)$  values by  $\chi(\text{obs}) = y\chi(\text{Yb}_2\text{O}_3) + (1-y)\chi(\text{intr})$ , where the impurity concentration  $y$  is adjusted such as to account for  $\chi(\text{obs})$  of the material investigated. As already mentioned above,  $\chi(\text{intr})$  is assumed to be temperature independent at sufficient low temperatures ( $T < 15$  K). This sort of analysis indicates that there are about 4% and 3%  $\text{Yb}_2\text{O}_3$  impurities in  $\text{YbCu}_{3.5}\text{Ga}_{1.5}$  and  $\text{YbCu}_4\text{Ga}$ , respectively. The corrected data are shown in Fig. 2 by solid symbols. To account for the susceptibility behavior in an extended temperature range, we have considered the interconfiguration fluctuation (ICF) model.<sup>19</sup> In the scope of this model,  $\chi(T)$  of Yb compounds follows from fluctuations between the magnetic  $4f^{13}$  and the nonmagnetic  $4f^{14}$  configuration. Therefore

$$\chi(T) = \frac{N\mu_{\text{eff}}^2 n_f}{3k_B(T + T_{sf})}. \quad (2)$$

The fractional valence (mean occupation of the  $4f$  shell)  $n_f$  follows from

$$n_f(T) = \frac{8}{8 + \exp[-E_{\text{ex}}/k_B(T + T_{sf})]}. \quad (3)$$

$\mu_{\text{eff}}$  is the effective magnetic moment associated with the total angular momentum  $j$  of the  $4f^{13}$  state ( $j = 7/2$ ) and  $E_{\text{ex}}$  is the energy difference of the  $4f^{14}$  and the  $4f^{13}$  state while  $T_{sf}$  is a characteristic temperature describing fluctuations between both states due to the

interaction with conduction electrons. If the energy of the  $4f^{13}$  state lies below that of the  $4f^{14}$  level, a modified Curie-Weiss law results. Otherwise,  $\chi(T)$  can vary from a Curie-Weiss law to a weakly temperature-dependent behavior, depending on the particular values of  $E_{ex}$  and  $T_{sf}$ .

Least squares fits according to the Eqs. (2) and (3) to the corrected data of both Yb compounds are shown as solid lines in Fig. 2, giving reasonable agreement. The obtained parameters are collected in Table I. The large negative values evaluated for  $E_{ex}$  clearly indicate that the magnetic  $4f^{13}$  state is situated well above the nonmagnetic  $4f^{14}$  ground state. A Curie-Weiss behavior is therefore expected only at elevated temperatures. The parameters observed for both compounds resemble those of well-known Yb compounds like  $\text{YbAl}_3$  or  $\text{YbC}_2$ .<sup>19</sup> The valence  $\nu_{ICF}$  ( $\nu = 2 + n_f$ ) which follows from the ICF model at room temperature [Eq. (3)] attains about 2.7 and 2.4 for  $\text{YbCu}_{3.5}\text{Ga}_{1.5}$  and  $\text{YbCu}_4\text{Ga}$ , respectively. It should be mentioned that similar to Ce compounds, Yb systems are constrained by the same numbers:  $0 \leq n_f \leq 1$ . However, instead of electron states, the  $f$  contribution is dominated from hole states.

Figure 3 shows  $L_{III}$ -absorption edge measurements of  $\text{YbCu}_4\text{Ga}$  and  $\text{YbCu}_3\text{Ga}_2$  at room temperature and at 10 K, respectively. Both spectra show two features around 8937 and 8943 eV corresponding to Yb being divalent and trivalent, respectively. The structure at 8937 eV is reinforced in the case of  $\text{YbCu}_4\text{Ga}$  as compared to  $\text{YbCu}_3\text{Ga}_2$  which is due to a higher concentration of the divalent state. We also notice that this structure still increases as the temperature is lowered from room temperature down to 10 K in both compounds, which establishes that the valence is temperature dependent, a characteristic of intermediate valence materials. After subtraction of the

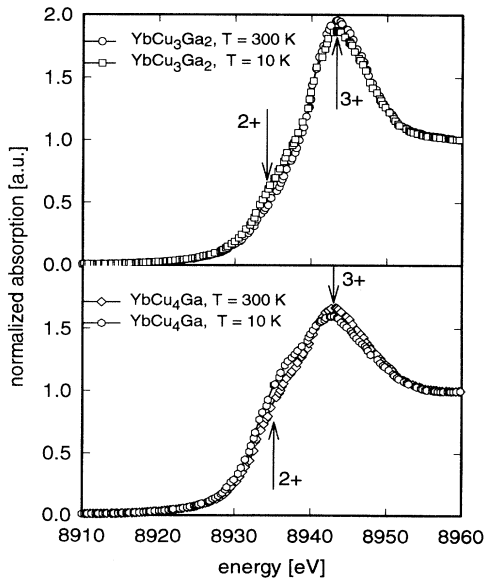


FIG. 3. X-ray absorption as a function of energy of  $\text{YbCu}_3\text{Ga}_2$  and  $\text{YbCu}_4\text{Ga}$  at  $T = 10$  and 300 K.

background in a standard manner, the edge was decomposed into a pair of Lorentzians ( $L1$  and  $L2$ ) and modified inverse tangent functions ( $AT1$  and  $AT2$ ) to provide the relative weight of the two electronic configurations and to evaluate the valence  $\nu_{L_{III}}$  of the Yb ions (Fig. 4). Thus we observed values of 2.62 and 2.92 for  $\text{YbCu}_4\text{Ga}$  and  $\text{YbCu}_3\text{Ga}_2$ , respectively. If  $y$  is the concentration of the  $\text{Yb}_2\text{O}_3$  impurity phase, the valence of the pure material  $\nu$  will be related to the valence  $\nu_{L_{III}}$  deduced from the  $L_{III}$  edge measurements by  $\nu = (\nu_{L_{III}} - 6y)/(1 - 2y)$ , as each Yb ion of  $\text{Yb}_2\text{O}_3$  will contribute to the 3+ peak. Using the values of the impurity concentration as observed from the susceptibility data and assuming a similar amount for  $\text{YbCu}_3\text{Ga}_2$ , reveals slightly reduced values, which are given in Table I.

As already inferred from the susceptibility measurements, the valence of the present Yb compounds increases with increasing Ga content and approaches an almost 3+ state for  $\text{YbCu}_3\text{Ga}_2$  at room temperature. However, when compared with the isomorphous compound  $\text{YbCu}_3\text{Al}_2$ , which exhibits at room temperature and at 10 K a valence  $\nu = 3.00$ ,<sup>21</sup> there is a distinct difference with appreciable consequences to physical properties. First of all, long-range magnetic order sets in below 2 K for  $\text{YbCu}_3\text{Al}_2$ , while no order has been observed down to 1.5 K at ambient pressure in the case of  $\text{YbCu}_3\text{Ga}_2$ . Additional differences arise from the fact that the paramagnetic Curie temperature  $\theta_p$  of  $\text{YbCu}_3\text{Ga}_2$  ( $\theta_p \approx -120$  K) is much larger than for  $\text{YbCu}_3\text{Al}_2$  [ $\theta_p \approx -17$  K (Ref. 12)]. The latter clearly indicates that the Kondo interaction strength  $k_B T_K \propto k_B |\theta_p|$  is larger in case of the Ga-substituted compounds; accordingly we suppose that the Yb moments are more screened due to a stronger  $s$ - $f$  hybridization. Thus the appearance of long-range magnetic order is much more unlikely and the slight deviation from the trivalent state follows consequently.

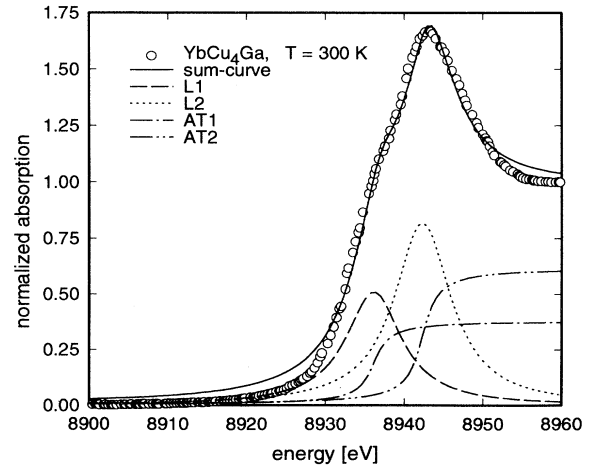


FIG. 4. X-ray absorption as a function of energy of  $\text{YbCu}_4\text{Ga}$  at  $T = 300$  K. The solid line is a fit according to two Lorentzian contributions ( $L1$  and  $L2$ ) and two modified inverse tangent functions ( $AT1$  and  $AT2$ ).

### B. Properties of $\text{YbCu}_{5-x}\text{Ga}_x$ at ambient pressure

The temperature dependence of the specific heat  $c_p$  for various compounds of the series  $\text{YbCu}_{5-x}\text{Ga}_x$  at temperatures up to 20 K is shown in Fig. 5. The contribution due to  $\text{Yb}_2\text{O}_3$ , showing an anomaly at about 2.2 K, has been subtracted; the concentration amounts to about 3%, which is of the same order as that derived from  $\chi(T)$ . As the substitution of Cu/Ga hardly changes the phonon contribution of  $c_p(T)$  in the medium-temperature range (20 K  $\leq T \leq$  80 K), only low-temperature data are presented in Fig. 5, where a significant increase of the heat capacity with increasing Ga content is observed. The phonon contribution to the heat capacity of all compounds between 10 K and 80 K can be reasonably described with a combination of one Debye function and two Einstein functions, where the characteristic temperatures  $\Theta_D = 127 \pm 3$  K,  $\Theta_{E_1} = 140 \pm 3$  K {6}, and  $\Theta_{E_2} = 265 \pm 5$  K {9} correspond to the 3 acoustic and 15 optical modes (the numbers of optical branches for the latter two Einstein temperatures are given in brackets).

Plotting the data as  $c_p/T$  vs  $T^2$  (inset, Fig. 5) reveals a continuous enhancement of the electronic contribution to the specific heat according to the rising Ga content. A polynomial extrapolation of  $c_p/T$  towards zero temperatures yields finally 180 mJ/molK<sup>2</sup> for  $\text{YbCu}_3\text{Ga}_2$  (compare Table I). Such a value of  $c_p/T$  resembles typical magnitudes of this quantity found for Yb-based Kondo lattices. For example, the compounds  $\text{YbCu}_4\text{Ag}$  (Ref. 2) and  $\text{YbCuAl}$  (Ref. 22) exhibit  $c_p/T$  values of 245 and 220 mJ/molK<sup>2</sup>, respectively. Extrapolating the data from the temperature range 10 K  $< T <$  20 K towards zero yields also a strong Ga-dependent increase of  $\gamma^{\text{HT}}$  from about 2 mJ/molK<sup>2</sup> for  $\text{YbCu}_5$  up to 63 mJ/molK<sup>2</sup> for  $\text{YbCu}_3\text{Ga}_2$ . The enhancement of  $c_p/T$  with increasing Ga content is concomitant with the change of the valency of the Yb ion towards the 3+ state.

Usually, the temperature-dependent specific heat of

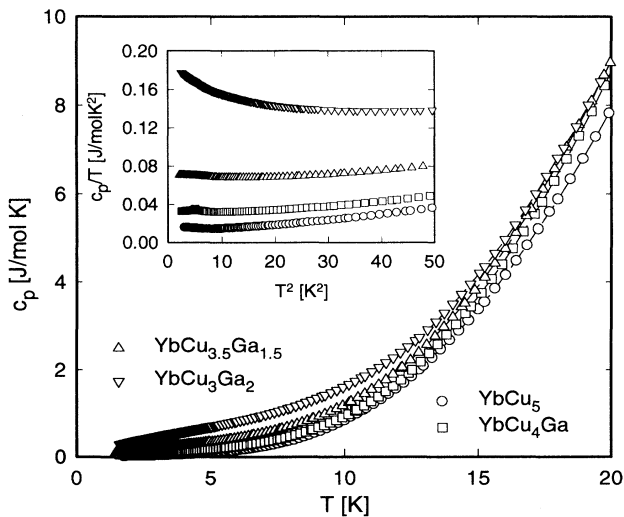


FIG. 5. Temperature-dependent specific heat  $c_p$  of various  $\text{YbCu}_{5-x}\text{Ga}_x$  compounds. The inset shows  $c_p/T$  vs  $T^2$ .

compounds in the proximity of the 3+ state may be described in terms of the Bethe-ansatz solution of the Coqblin-Schrieffer model. Assuming that for the compound  $\text{YbCu}_3\text{Ga}_2$  crystal field splitting is of minor importance, at least at ambient pressure, the characteristic temperature of the system  $T_0$  ( $T_0 = T_K/W_j$ , where  $W_j$  is the Wilson number<sup>23</sup>) can be evaluated from the specific heat data in the zero temperature limit by<sup>24</sup>

$$c/T(T \rightarrow 0) \equiv \gamma = \frac{(N-1)\pi R}{6T_0}, \quad (4)$$

with  $R$  the gas constant and  $N$  the degeneracy of the Yb moments ( $N = 2j + 1$ ). With  $\gamma \approx 180$  mJ/molK<sup>2</sup> and  $j = 7/2$ ,  $T_0$  is found to be about 170 K. The large  $T_0$  value, which is of the same order of magnitude as the paramagnetic Curie temperature  $|\theta_p| \approx 120$  K, implies that the Kondo interaction strength  $k_B T_K$  is much larger than RKKY interaction in this compound. The latter energy scale is usually obtained by a scaling of the transition temperatures of the respective rare earth compounds according to the de Gennes factor, yielding typical ordering temperatures of Yb compounds without the Kondo effect of about 1–10 K [ $\text{GdCu}_3\text{Ga}_2$ :  $T_N = 12$  K (Ref. 25)]. Since  $T_K \gg T_{\text{RKKY}}$ , no long-range magnetic order can be expected for  $\text{YbCu}_3\text{Ga}_2$ . If Eq. (4) is also applied to the compounds  $x = 1.5$  and  $x = 1$ , an even larger characteristic temperature  $T_0$  of the order of several hundreds of kelvin can be deduced.

Due to the fact that the valency  $\nu$  of the Yb ion, even in the case of  $\text{YbCu}_3\text{Ga}_2$ , deviates from 3, Eq. (4) may not fully account for the low-temperature behavior of  $c_p(T)$ . However, Bickers *et al.*<sup>26</sup> have calculated the temperature-dependent specific heat for fixed values of the degeneracy  $N$  while the mean occupation of the  $f$ -shell  $n_f$  has been used as parameter. The results of Bickers *et al.*<sup>26</sup> show that for a rather extended temperature range the theoretical  $c_p(T)$  behavior does not depend sensitively on  $n_f$  if the value of  $n_f$  is kept in a limited range. However, for  $T \ll T_0$  and  $n_f < 1$ , the calculated behavior of  $c_p(T)$  deviates from the case  $n_f = 1$ . Both larger and smaller  $c_p(T)$  values may occur, depending on the particular choice of  $n_f$ .

On the other hand, if crystal field splitting acts on the  $j = 7/2$  state of the Yb ion, due to the hexagonal symmetry, a doublet as the ground state is expected. This case is probably of importance for  $\text{YbCu}_3\text{Ga}_2$ , at least at somewhat elevated values of pressure. For a doublet as the ground state, the Kondo temperature  $T_K$  follows from<sup>27</sup>  $c_p/T(T \rightarrow 0) = 0.68R/T_K$ , yielding  $T_K \approx 31$  K for  $\text{YbCu}_3\text{Ga}_2$ . Even this value is rather large, and a nonmagnetic ground state is therefore likely.

The temperature-dependent resistivity  $\rho$  of various  $\text{YbCu}_{5-x}\text{Ga}_x$  compounds is shown in Fig. 6. Starting with  $\text{YbCu}_5$ , a gradual change of the resistivity behavior is observed. (i) The residual resistivity  $\rho_0$  increases from about 4 to 85  $\mu\Omega$  cm with growing Ga content. As the residual resistivity arises mainly from scattering processes of conduction electrons on static imperfections, we attribute this increase to a partial disorder within the crystallographic unit cell. As mentioned above, the substitution of Cu by Ga takes place preferentially at the

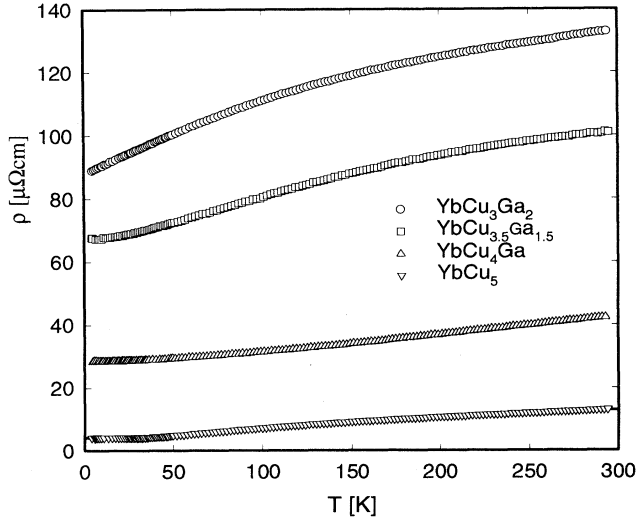


FIG. 6. Temperature dependence of the electrical resistivity  $\rho$  of various  $\text{YbCu}_{5-x}\text{Ga}_x$  compounds.

3(*g*) sites of the hexagonal unit cell. Since a compound with the nominal composition  $\text{YbCu}_2\text{Ga}_3$  cannot be obtained, all the Ga-substituted compounds show partial disorder. However, it is noted that all the Yb ions as well as the Cu ions on the 2(*c*) sites exhibit full structural order. Besides substitutional disorder, parts of the observed increase of  $\rho_0$  may be inferred from an increasing contribution of magnetic scattering processes. (ii) While  $\rho(T)$  of  $\text{YbCu}_5$  shows an almost linear temperature dependence at elevated temperatures, the increasing Ga content causes a pronounced negative curvature of  $\rho(T)$ . This change may be explained by the growing importance of the interactions of conduction electrons with the magnetic moment of the Yb ions. Due to the divalency of the Yb ion, it is expected that  $\text{YbCu}_5$  behaves like earth-alkali compounds. Thus,  $\rho(T)$  should be similar to that of simple metals and compounds. To prove this assumption quantitatively, we describe  $\rho(T)$  with a modified Bloch-Grüneisen law:<sup>28,29</sup>

$$\rho_{\text{ph}}(T) = 4R\Theta_D \left( \frac{T}{\Theta_D} \right)^5 \int_0^{\Theta_D/T} \frac{z^5 dz}{\exp(z) - 1} (1 - \exp(-z)) - KT^3. \quad (5)$$

Equation (5) takes into account the Debye temperature  $\Theta_D$ , a temperature-independent constant  $R$  proportional to the electron-phonon interaction strength and, additionally, the constant  $K$ , related to scattering processes of the conduction electrons on a narrow band in the proximity to the Fermi energy. A least squares fit according to Eq. (5) yields a rather good agreement with the experimental data (solid line, Fig. 6). The parameters evaluated are  $R = 8 \mu\Omega \text{cm K}^{-1}$ ,  $\Theta_D = 210 \text{ K}$ , and  $K = 1.0 \times 10^{-7} \mu\Omega \text{cm K}^{-3}$ . The overall value of  $\Theta_D$  is in agreement with the characteristic temperatures derived from  $c_p(T)$  ( $\Theta_D = 127 \text{ K}$ ,  $\Theta_{E_1} = 140 \text{ K}$ , and

$\Theta_{E_2} = 265 \text{ K}$ ) and indicates a rather soft lattice.

However, this simple behavior progressively breaks down as one proceeds to  $\text{YbCu}_3\text{Ga}_2$  and the resistivity can no longer be accounted for in the scope of Eq. (5). As provided from susceptibility and  $L_{\text{III}}$ -absorption edge measurements, the Yb ions change their magnetic state upon the Ga substitution. If eventually  $(1 - n_f) \ll 1$  is achieved for  $\text{YbCu}_3\text{Ga}_2$ , Kondo scattering processes become important. The associated hybridization of conduction electrons with the  $4f^{13}$  states appears to be very strong at ambient pressure, yielding the large deduced values of the Kondo temperature  $T_K$ , and prevents long-range magnetic order originating from the RKKY interaction.

Figure 7 shows the temperature-dependent thermopower  $S(T)$  of  $\text{YbCu}_{5-x}\text{Ga}_x$ . Common to all the investigated compounds is the negative sign of  $S(T)$  in the whole temperature range. In contrast to cerium compounds where the Kondo effect yields positive thermopower values, at least at elevated temperatures, the negative sign of  $S(T)$  is observed in most of the Yb-based Kondo systems. Theoretically, the opposite-sign behavior of cerium and ytterbium compounds follows from the electron-hole symmetry of the  $4f^1$  and the  $4f^{13}$  states, since the derivative of the electronic density of states at the Fermi level determines the sign of thermopower.

The overall  $S(T)$  behavior of  $\text{YbCu}_{5-x}\text{Ga}_x$  is characterized by shallow minima, whereas the minimum temperature decreases along with increasing Ga content. Simultaneously, the absolute  $S(T)$  values grow. The observed large values, particularly for  $\text{YbCu}_3\text{Ga}_2$ , are attributed to the Kondo interaction, yielding to  $S(T)$  values which exceed those of simple metals by one or two orders of magnitude. Considering only the Kondo effect in a metallic system,  $S(T)$  is characterized by a universal behavior and extremely large values, which are determined by a single temperature scale, the Kondo temper-

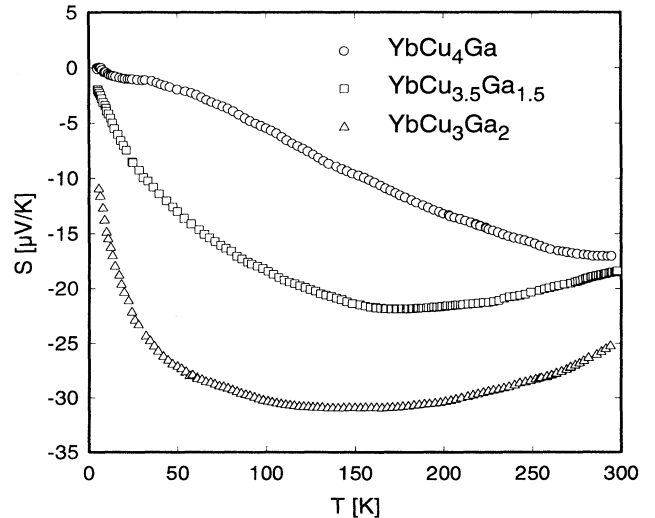


FIG. 7. Temperature dependence of the thermopower  $S$  of various  $\text{YbCu}_{5-x}\text{Ga}_x$  compounds.

ature  $T_K$ . However, when other interaction mechanisms like the RKKY interaction or crystal field splitting become comparable to the Kondo interaction, the proposed universal behavior can no longer be observed. Instead, either pronounced minima followed by maxima, or vice versa, usually occur.<sup>39</sup> The absence of long-range magnetic order in  $\text{YbCu}_{5-x}\text{Ga}_x$  follows also from the absence of a positive  $S(T)$  contribution at low temperatures. As has been shown already by Fischer,<sup>40</sup> the sign of the thermopower for Kondo compounds at low temperatures is determined from a mutual balance of RKKY and Kondo interactions. In the case of Yb systems, the former interaction yields a positive  $S(T)$  contribution, while the latter mechanism is responsible for negative  $S(T)$  values. The resulting sign of  $S(T)$  follows then from whichever process dominates the other. In the scope of this model, the observed  $S(T)$  behavior of  $\text{YbCu}_{5-x}\text{Ga}_x$  confirms the absence of long-range magnetic order, together with the other experiments performed in this study.

### C. Pressure response of $\text{YbCu}_{5-x}\text{Ga}_x$

Previously, it has been demonstrated that the application of hydrostatic pressure reduces the Kondo temperature of ytterbium systems and accordingly favors increasing magnetic interactions.<sup>6,9,30,31</sup> Such a pressure-induced change of the magnetic state will be demonstrated below in detail for two compounds of the series, namely,  $\text{YbCu}_4\text{Ga}$  and  $\text{YbCu}_3\text{Ga}_2$ .

Figure 8 shows  $\rho(T)$  of  $\text{YbCu}_4\text{Ga}$  at various values of applied pressure in a normalized representation. At ambient pressure,  $\rho(T)$  increases continuously with temperature, implying that magnetic scattering processes are of minor importance. As pressure grows, magnetic scattering processes become more dominant, giving rise to remarkable structure in the  $\rho(T)$  curves. Approximately beyond 60 kbar, a maximum in  $\rho(T)$  develops, where the

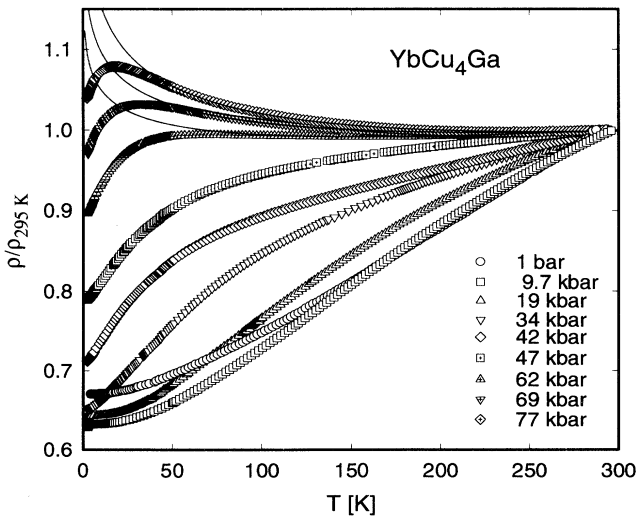


FIG. 8. Temperature- and pressure-dependent electrical resistivity  $\rho$  of  $\text{YbCu}_4\text{Ga}$  plotted in a normalized representation.

temperature of this maximum,  $T_\rho^{\text{max}}$ , shifts to lower values. Finally, at  $p = 77$  kbar, the maximum centers at  $T_\rho^{\text{max}} \approx 17$  K. Above  $T_\rho^{\text{max}}$  the behavior of the resistivity is dominated by a negative logarithmic contribution. This distinct temperature dependence is usually taken as an archetypal sign of Kondo interactions. A confirmation for the occurrence of this type of interaction follows from a fit to the data, considering the most dominant scattering processes in this compound and their contributions to  $\rho(T)$ . Based on Matthiessen's rule, the resistivity can be accounted for by a sum of the temperature-independent residual resistivity  $\rho_0$ , the phonon interaction term  $\rho_{\text{ph}}$ , and the logarithmic Kondo contribution  $\rho_{\text{mag}}$ , i.e.,

$$\rho(T) = \rho_0 + \rho_{\text{ph}}(T) + \rho_{\text{mag}}(T) = a + \rho_{\text{BG}}(T) - c \ln(T). \quad (6)$$

$\rho_{\text{BG}}(T)$  reflects a phonon contribution according Eq. (5). The results of a least squares fit at higher temperatures based on Eq. (6) are shown as solid lines in Fig. 8, confirming the importance of the Kondo effect. The negative logarithmic contribution due to scattering processes on independently acting scattering centers is expected to occur only at elevated temperatures. At low temperatures, the properties owing to the sublattice of Yb ions become prominent. In case of the periodic arrangement of almost magnetic Yb ions, the conduction electrons can move as Bloch waves. The associated resistivity contribution reduces and finally approaches zero at zero temperatures. In this case,  $\rho(T)$  is characterized by a behavior proportional to  $T^2$  at low temperatures, yielding a maximum at  $T_{\text{max}}^\rho \approx T_K$  since only at elevated temperatures does the typical Kondo contribution to the resistivity occur. The distinct resistivity behavior of Kondo lattices has also been shown from calculations based on solutions of the periodic version of the Anderson model.<sup>32-37</sup> In the scope of these calculations it can be concluded that  $T_K$  of  $\text{YbCu}_4\text{Ga}$  decreases along with increasing pressure, approaching a value of roughly 20 K at  $p = 77$  kbar. However, a substantial reduction of  $\rho(T)$  and a clear  $T^2$  behavior at the lowest temperatures as in classical Kondo lattice systems like  $\text{CeAl}_3$ ,  $\text{CeCu}_6$ , or  $\text{YbCu}_4\text{Ag}$  could not be resolved, the reason of which is supposed to arise from partial disorder of the Ga ions on the  $3(g)$  sites of the hexagonal unit cell. This causes a nonuniform chemical and therefore electrical surrounding in the Yb sites. Such a situation can give rise to faults in the Bloch-like motion of the conduction electrons; consequently the resistivity stays relatively large. Taking the maximum in  $\rho$  vs  $T$  as a measure of  $T_K$ , we can estimate a Grüneisen parameter  $\Omega_i$ , expressing the volume dependence of various characteristic temperatures ( $T_i$ ). From the pressure-dependent variation of  $T_K$  the electronic Grüneisen parameter  $\Omega_e$  is obtained as  $\Omega_e = -\partial(\ln T_K)/\partial(\ln V) = (B_0/T_K)(\partial T_K/\partial p)$ . Since the bulk modulus  $B_0$  of  $\text{YbCu}_4\text{Ga}$  is not yet known, we use  $B_0$  of the compound  $\text{YbCu}_4\text{Ag}$  (Ref. 6) as a first approximation. This choice seems to be justified by the fact that the pressure- and temperature-dependent variation of the electrical resistivity nearly resembles the behavior of  $\text{YbCu}_4\text{Ga}$ .<sup>6</sup> Using  $\partial T_K/\partial p|_{p \geq 62 \text{ kbar}} \approx -3.3 \text{ K/kbar}$ ,

one arrives finally at  $\Omega_e|_{p=62 \text{ kbar}} \approx -50$ .

Usually heavy fermion compounds based on cerium or uranium and characterized by low values of  $T_K$  exhibit large positive values of  $\Omega_e$  (of the order of 100), implying that volume plays an essential role for electronic properties of the system. On the contrary, Yb systems that have studied show negative values of  $\Omega_e$ , resulting from the fact that  $\partial T_K / \partial p < 0$ .

A qualitatively different pressure response has been obtained for  $\text{YbCu}_3\text{Ga}_2$ . In Fig. 9 the electrical resistivity of  $\text{YbCu}_3\text{Ga}_2$  is plotted as a function of temperature for various values of pressure. Starting at ambient pressure,  $\rho(T)$  increases with a negative slope up to room temperature. If pressure is applied to this compound, a minimum roughly at 25 K starts to develop, becoming more pronounced as the pressure further increases. Below this minimum, an almost negative logarithmic behavior of the resistivity clearly indicates Kondo interaction. Due to the fact that the Kondo interaction strength in Yb compounds weakens as the pressure rises, the relation between  $k_B T_K$  and the crystal field splitting  $\Delta_{\text{CEF}}$  may become reverse in  $\text{YbCu}_3\text{Ga}_2$ . At ambient pressure it is expected that  $k_B T_K > \Delta_{\text{CEF}}$ , causing crystal field splitting not to dominate the ground state properties. However, at the largest values of applied pressure,  $T_K$  is supposed to be drastically diminished, yielding  $k_B T_K < \Delta_{\text{CEF}}$ . The resistivity behavior of the latter case can be described in terms of the model of Cornut and Coqblin.<sup>38</sup> This model yields a logarithmic resistivity behavior in the crystal field ground state and usually a  $-\ln(T)$  term for temperatures above the uppermost crystal field level. Moreover, these logarithmic ranges are separated by a smooth maximum in the vicinity of the overall crystal field splitting. This distinct  $\rho(T)$  de-

pendence is easy to observe for  $p = 57$  and  $64$  kbar. Again, a test of this model can be achieved at low and at high temperatures considering the different contributions of Eq. (6). A least squares fit to the results of the  $p = 64$  kbar  $\rho(T)$  measurement is shown as a solid line in Fig. 9, revealing good agreement with the experiment below and above the maximumlike feature around 75 K. The Debye temperature  $\Theta_D$  evaluated from this fit is about 130 K, i.e., much lower than that deduced for  $\text{YbCu}_5$ . The inset in this figure shows the pressure-dependent variation of the room temperature resistivity. Contrary to the case of Ce compounds, the resistivity decreases as the pressure rises. According to the expression of Cornut and Coqblin,<sup>38</sup> the magnitude of the absolute resistivity depends on the parameter  $JN(E_F)$  [ $J$  is the  $s$ - $f$  coupling constant;  $N(E_F)$  is the electronic density of states at the Fermi energy]; a decrease of the resistivity is synonymous with a decrease of  $JN(E_F)$ . This change of  $JN(E_F)$  is confirmed also by a decrease of  $T_K$  as a general trend in Yb systems when pressure is applied.

#### IV. SUMMARY

A comprehensive investigation of the series  $\text{YbCu}_{5-x}\text{Ga}_x$  ( $0 \leq x \leq 2$ ) indicates that due to the Cu/Ga substitution the valence of the Yb ion is driven from a divalent state in  $\text{YbCu}_5$  to a nearly trivalent state in  $\text{YbCu}_3\text{Ga}_2$ . Since the Cu/Ga substitution causes an enlargement of the hexagonal unit cell, chemical pressure cannot be made responsible for the observed change of the valence and therefore of the magnetic state. Rather, it has to be anticipated that this crossover is of electronic origin.

In spite of the fact that susceptibility measurements performed on  $\text{YbCu}_3\text{Ga}_2$  revealed an effective moment, almost equal to that of an  $\text{Yb}^{3+}$  ion, the trivalent state has not been fully developed. This clearly follows from  $L_{\text{III}}$ -absorption edge measurements at high and at low temperatures and is supported by the rather large value of  $c_p/T$  of about  $180 \text{ mJ/mol K}^2$ . The small deviation from the trivalent state, in our opinion, is also obvious from the resistivity measurements. At ambient pressure,  $\rho(T)$  does not exhibit those typical features, like negative logarithmic contributions, which are usually present in classical Kondo systems. Moreover, the crystal field splitting seems to be of minor importance, since  $\rho(T)$  of all the compounds investigated does not show a spin disorder contribution associated with the thermal population of the different crystal field levels above the ground state.<sup>38,41</sup>

Resistivity measurements at elevated pressure, particularly in the case of  $\text{YbCu}_3\text{Ga}_2$ , show clearly the influence of the crystal field splitting, since two negative logarithmic resistivity contributions are present, which are separated from a local maximum, staying nearly constant as the pressure increases.

The series  $\text{YbCu}_{5-x}\text{Ga}_x$  can therefore be used to study

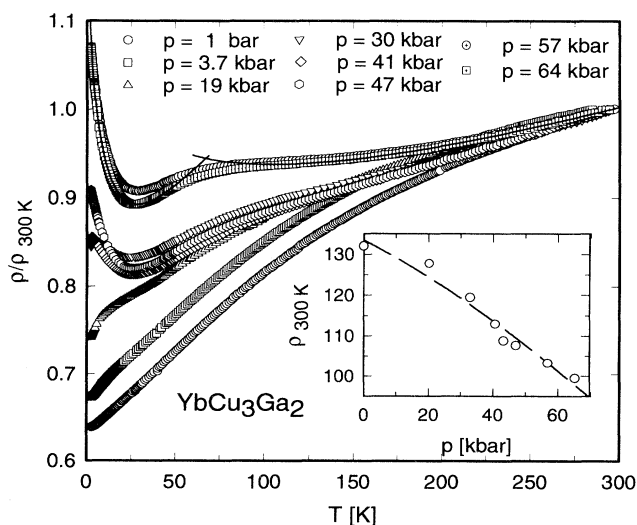


FIG. 9. Temperature- and pressure-dependent electrical resistivity  $\rho$  of  $\text{YbCu}_3\text{Ga}_2$  plotted in a normalized representation. The inset shows the pressure-dependent variation of the room temperature resistivity.

step by step the increase of the valency  $\nu$  of the Yb ion due to the Cu/Ga substitution. Associated with rising values of  $\nu$  are increasing magnetic interactions. However, a magnetic instability was not observed, thought to be prevented by strong Kondo interactions.

#### ACKNOWLEDGMENTS

Parts of this work have been supported by the Austrian Science Foundation, Project Nos. P 7608 and P 10269. We are grateful to A. Markosyan for helpful discussions.

- <sup>1</sup> A. Iandelli and A. Palenzona, *J. Less-Common. Met.* **25**, 333 (1987).
- <sup>2</sup> C. Rossel, K.N. Yang, M.B. Maple, Z. Fisk, E. Zirngiebl, and J.D. Thompson, *Phys. Rev. B* **35**, 1914 (1987).
- <sup>3</sup> M.J. Besnus, P. Haen, N. Hamdaoui, A. Herr, and A. Meyer, *Physica B* **163**, 571 (1990).
- <sup>4</sup> G. Polatsek and P. Bonville, *Z. Phys. B* **88**, 189 (1992).
- <sup>5</sup> P. Schlottmann, *J. Appl. Phys.* **73**, 5412 (1993).
- <sup>6</sup> E. Bauer, R. Hauser, E. Gratz, K. Payer, G. Oomi, and T. Kagayama, *Phys. Rev. B* **48**, 15873 (1993).
- <sup>7</sup> M.J. Besnus, A. Braghta, N. Hamdaoui, and A. Meyer, *J. Magn. Magn. Mater.* **104 & 107** 1385 (1992).
- <sup>8</sup> B. Bonville, B. Canaud, J. Hammann, J.A. Hodges, P. Imbert, G. Jehanno, A. Severing, and Z. Fisk, *J. Phys. (France) I* **2**, 459 (1992).
- <sup>9</sup> E. Bauer, E. Gratz, R. Hauser, A. Galatanu, A. Kottar, H. Michor, W. Perthold, T. Kagayama, G. Oomi, N. Ichimiya, and S. Endo, *Phys. Rev. B* **50**, 9300 (1994).
- <sup>10</sup> D.T. Adroja, S.K. Malik, B.D. Padalia, and R. Vijayaraghavan, *J. Phys. C* **20**, L307 (1987).
- <sup>11</sup> E. Bauer, K. Payer, R. Hauser, E. Gratz, D. Gignoux, D. Schmitt, N. Pillmayr, and G. Schaudy, *J. Magn. Magn. Mater.* **104 - 107**, 651 (1992).
- <sup>12</sup> E. Bauer, R. Hauser, E. Gratz, D. Schmitt, and D. Gignoux, *J. Phys. Condens. Matter.* **4**, 7829 (1992).
- <sup>13</sup> E. Bauer, E. Gratz, L. Keller, P. Fischer, and A. Furrer, *Physica B* **186 - 188**, 608 (1993).
- <sup>14</sup> B.M. Stelmakhovich, Yu.B. Kuz'ma, and V.S. Babizhet'sky, *J. Alloys Compounds* **190**, 161 (1993).
- <sup>15</sup> L. Keller, Ph.D. thesis, ETH Zürich, 1994.
- <sup>16</sup> A. Eiling and J. Schilling, *J. Phys. F* **11**, 623 (1981).
- <sup>17</sup> J.C.P. Klaase, J.W.E. Sterkenburg, A.H.M. Bleyendaal, and F.R. de Boer, *Solid State Commun.* **12**, 561 (1973).
- <sup>18</sup> J.C.P. Klaase, F.R. de Boer, and P.F. de Chatel, *Physica B* **106**, 178 (1981).
- <sup>19</sup> B. Sales and D. Wohlleben, *Phys. Rev. Lett.* **35**, 1240 (1975).
- <sup>20</sup> A.C. Hewson, *The Kondo Problem to Heavy Fermions*, Cambridge Studies in Magnetism, Vol. 2 (Cambridge University Press, Cambridge, England, 1993).
- <sup>21</sup> C. Godart and E. Alleno (unpublished).
- <sup>22</sup> A. Bleckwedel, A. Eichler, and R. Pott, *Physica B* **107**, 93 (1981).
- <sup>23</sup> A.C. Hewson and J.W. Rasul, *J. Phys. C* **16**, 6799 (1983).
- <sup>24</sup> V.T. Rajan, *Phys. Rev. Lett.* **51**, 308 (1983).
- <sup>25</sup> E. Bauer (unpublished).
- <sup>26</sup> N.E. Bickers, D.L. Cox, and J.W. Wilkins, *Phys. Rev. B* **54**, 230 (1987).
- <sup>27</sup> L.N. Oliveira and J. Wilkins, *Phys. Rev. Lett.* **47**, 1553 (1981).
- <sup>28</sup> G. Grimvall, *The Electron-Phonon Interaction in Metals* (North-Holland, Amsterdam, 1981).
- <sup>29</sup> N.F. Mott and H. Jones, *The Theory of the Properties of Metals and Alloys* (Oxford University Press, London, 1958).
- <sup>30</sup> J.D. Thompson, in *Frontiers in Solid State Sciences*, edited by L.C. Gupta and M.S. Multani (World Scientific, London, 1993), Vol. 2, p. 107.
- <sup>31</sup> G. Sparn and J.D. Thompson, *J. Alloys Compounds* **181**, 197 (1992).
- <sup>32</sup> N. Grewe and T. Pruschke, *Z. Phys. B* **60**, 311 (1985).
- <sup>33</sup> A. Yoshimori and H. Kasai, *J. Magn. Magn. Mater.* **31 - 34**, 475 (1983).
- <sup>34</sup> P. Coleman, *J. Magn. Magn. Mater.* **63 - 64**, 245 (1987).
- <sup>35</sup> D.L. Cox and N. Grewe, *Z. Phys. B* **71**, 321 (1988).
- <sup>36</sup> K.H. Fischer, *Z. Phys. B* **74**, 475 (1989).
- <sup>37</sup> J. Schilling, *Phys. Rev. B* **33**, 1667 (1986).
- <sup>38</sup> D. Cornut and B. Coqblin, *Phys. Rev. B* **5**, 4541 (1972).
- <sup>39</sup> E. Bauer, *Adv. Phys.* **40**, 417 (1991).
- <sup>40</sup> K.H. Fischer, *Z. Phys. B* **76**, 315 (1989).
- <sup>41</sup> S. Maekawa, S. Kashiba, S. Takahashi, and M. Tachiki, in *The Theory of Heavy Fermions and Valence Fluctuations*, Springer Series in Solid State Sciences, Vol. 62, edited by T. Kasuya and T. Saso (Springer, Berlin, 1985), p. 90.